

## Article

# Optimization of Land Use Structure Based on the Coupling of GMOP and PLUS Models: A Case Study of Lvliang City, China

Zhen Wang <sup>†</sup>, Anya Zhong <sup>†</sup> and Quanzhi Li <sup>\*†</sup> 

School of Geographical Sciences and Surveying Engineering, China University of Mining and Technology, Beijing 100083, China

\* Correspondence: bqt2300204053@student.cumtb.edu.cn

<sup>†</sup> These authors contributed equally to this work.

**Abstract:** Reasonable land use planning and management efficiently allocates land resources, promotes socio-economic development, protects the ecological environment, and fosters sustainable development. It is a crucial foundation for achieving harmonious coexistence between humans and nature. Optimizing land use is key to land use planning and management. Four scenarios are established: an economic development scenario (EDS), an ecological protection scenario (EPS), a natural development scenario (NDS), and a coordinated development scenario (CDS). This study simulates land use patterns under these scenarios through the coupling of the GMOP and PLUS models. It analyzes the land use efficiency transformation index, landscape ecological index, comprehensive land use benefits, and ecosystem service value (ESV) for each pattern. The optimal land use pattern is determined by balancing these factors. The results indicated that under the CDS, the areas of wasteland, grassland, forest land, water bodies, construction land, and unused land in Lvliang City were 6724.29 km<sup>2</sup>, 6664.74 km<sup>2</sup>, 6581.84 km<sup>2</sup>, 126.94 km<sup>2</sup>, 1017.33 km<sup>2</sup>, and 0.42 km<sup>2</sup>, respectively. This represented the optimal land use plan for Lvliang City. The plan minimized human interference with the landscape pattern, achieved the highest land use efficiency transformation index, and reached a reasonable balance between land use benefits and ESV. The research findings provide valuable insights and decision support for regional land use planning, territorial space planning, and related policy formulation.

**Keywords:** land use optimization; MOP model; PLUS models; ecosystem service values; Lvliang city



**Citation:** Wang, Z.; Zhong, A.; Li, Q. Optimization of Land Use Structure Based on the Coupling of GMOP and PLUS Models: A Case Study of Lvliang City, China. *Land* **2024**, *13*, 1335. <https://doi.org/10.3390/land13081335>

Academic Editors: Jūratė Sužiedelytė-Visockienė and Bindong Sun

Received: 15 July 2024

Revised: 16 August 2024

Accepted: 21 August 2024

Published: 22 August 2024



**Copyright:** © 2024 by the authors. Licensee MDPI, Basel, Switzerland. This article is an open access article distributed under the terms and conditions of the Creative Commons Attribution (CC BY) license (<https://creativecommons.org/licenses/by/4.0/>).

## 1. Introduction

China possesses extensive land resources; however, the significant population leads to a limited availability of land per capita. Additionally, inefficiencies in land use structures are evident, manifesting as low land use efficiency, loss of farmland, and an imbalance between urban and rural land distribution [1–3]. The land use structure illustrates the distribution and proportion of diverse land use types within a defined area, thereby reflecting the composition of land designated for various purposes in a specific spatial context. An inadequate land use structure directly hinders regional economic development and disrupts the harmonious functioning of ecosystems, thereby affecting the sustainability of the region [4]. Land use structure optimization involves the utilization of scientific methodologies to improve the allocation and management of finite land resources. This process requires the consideration of multiple development objectives and strives to attain an optimal balance among different regions and land uses. By doing so, the efficiency of land resource utilization is enhanced, the ecological environment is preserved, the quality of life for residents is improved, and sustainable development is promoted across economic, social, and environmental dimensions [5,6]. With the rapid progression of urbanization, land utilization and development are essential components of urban construction. Nevertheless, the intensification of land development inevitably exerts a negative impact on

the environment. Activities such as deforestation, the encroachment on farmland, overgrazing, and coal mining significantly disrupt the balance between economic advancement and environmental conservation [7–10]. Severe impacts on the ecosystem are inevitably caused by inefficient land use, and significant depletion of ESV is likewise occasioned by excessive land development and inappropriate land use type conversions. The conflict between economic development and environmental preservation is mitigated through the optimization of land use structures and layouts. This approach simultaneously addresses multiple objectives, such as promoting economic growth, ensuring ecological protection, and fostering social harmony, thus contributing to sustainable regional development.

There has been extensive research on land use optimization both domestically and internationally. Land use structure optimization is primarily divided into quantitative structure optimization and spatial layout simulation optimization [11,12]. The main tools for quantitative structure optimization include GM (1, 1), system dynamics models, and Markov chains. However, these models have drawbacks such as high data requirements, simple model assumptions, sensitivity to external factors, and limited prediction ranges [13–15]. The GMOP model, on the other hand, can simultaneously consider multiple objectives and factors, has strong data processing capabilities and flexibility, and can simulate land use changes under different policy implementations, providing more scientific and reasonable predictions for land use planning [16,17]. Many scholars have conducted extensive research on using GMOP for land use structure optimization. For example, Zhu et al. [18] developed a multi-objective, constrained regional land use structure model known as PLUS-GMOP, in which three scenarios were hypothesized. This model facilitated the selection of the optimal land use strategy for the Wuhan metropolitan area, providing an innovative technical framework for the sustainable development of large urban regions; Li et al. [19] developed a grey linear programming optimization model designed to improve the land use structure in the Sichuan–Yunnan ecological barrier region. This model aimed to maximize ecological value while also enhancing economic benefits, utilizing the current land use conditions in the study area. This approach offered a clear methodology for optimizing ecological service value within large ecological functional zones; Mo et al. [20] employed the gray linear multi-objective programming approach, framed within the context of production–living–ecological space (PLES), to develop the GMOP-Markov-PLUS model. This model effectively predicted future land use patterns across various scenarios. Additionally, it proposed three distinct long-term land use strategies for the study area, which included considerations for ecological conservation, economic growth, and sustainable development prospects.

Multi-objective linear programming effectively addresses the quantitative aspects of land use optimization, generating appropriate schemes for land use quantities. The predominant models for simulating land structure optimization scenarios currently encompass the CA–Markov model [21], the CLUES model [22], and the FLUS model [23]. Nonetheless, these models are encumbered by challenges such as low spatial resolution, omission of local details, inadequate local adaptability of model parameters, and an absence of dynamic adaptability. While they attain high precision in simulations of small-scale land use, their performance is diminished in larger-scale simulations. The PLUS model primarily functions as a simulation tool for forecasting future alterations in land use. It integrates a module for analyzing land expansion strategies along with a cellular automata model that is influenced by various classes of stochastic patch seeds. It is distinguished by its user-friendly interface and simplicity of operation. The PLUS model is particularly effective for large-scale regional land use simulations. Its integration with GIS enables a detailed analysis of spatial heterogeneity, characteristics, and temporal dynamics within land use structures. As a result, this integration significantly improves the optimization of spatial configurations in land use patterns [24,25].

As urban development progresses and various social factors drive change, the pattern of land use is becoming increasingly complex and uncertain, making the study of land use structure optimization a hot topic. Zhong et al. [26] combined the GMOP and PLUS

models, considering the existing land use layout and policy constraints, and concluded that the land pattern under the balanced development (BD) scenario ensured economic growth without compromising ecological benefits. Shu et al. [27] employed the ESV, GMOP, and PLUS models to forecast land use changes and ESV across various development scenarios. Their findings indicated that the sustainable development (SD) scenario was likely more appropriate for future regional advancements. While the ESV was marginally lower compared to the ecological land protection (ELP) scenario, there was a notable increase in economic benefits. Luan et al. [28] conducted simulations of land use patterns across different scenarios by integrating the NSGA-II and PLUS models. Their analysis revealed that the most significant variations among the scenarios were predominantly observed in the areas designated for forest land and cultivated land. Meng et al. [29] utilized a combination of the GMOP and PLUS models to simulate land use configurations across four distinct scenarios. Their analysis focused on changes in ecological benefits, economic advantages, and carbon emissions, enabling the identification of the most favorable land use arrangement.

Previous studies primarily used the PLUS model to simulate land use configurations under various development scenarios, and then conducted a basic analysis of ecosystem service value (ESV) and land use benefits to identify the optimal land use structure. However, these studies did not examine the conversion efficiency between ESV and land use benefits as land use patterns evolved, nor did they account for the impact of changing land use patterns on landscape configurations. This study is based on the coupling of the GMOP and PLUS models, establishing different scenarios and constraints to predict the land use structure of Lvliang City in 2035. A land use benefit conversion index is constructed to explore the conversion efficiency between land use benefits and ESV during the transition from the current land use pattern to future patterns. The sustainable development potential is evaluated under various development scenarios, and the optimal land use structure for Lvliang City is determined through a comprehensive analysis of the land use benefit conversion index, land use benefits, landscape pattern indices, and ESV across different scenarios.

## 2. Study Area and Data Sources

### 2.1. Study Area

Lvliang City, a prefecture-level city under the administration of Shanxi Province, boasts abundant mineral resources and favorable metallogenic conditions, with coal, iron, and dolomite being the primary minerals (Figure 1). It is distinguished by multiple metallogenic epochs, extensive distribution, varied mineral types, significant reserves, superior quality, and ease of extraction. Spanning latitudes from 36°43' to 38°43' North and longitudes from 110°22' to 112°19' East, Lvliang City is adjacent to Taiyuan and Jinzhong in the east, separated from Shaanxi Province by the Yellow River to the west, and borders Linfen and Xinzhou to the south and north, respectively, with a total area of 21,000 square kilometers. The city possesses a favorable climate, with local economic development primarily dependent on activities such as coal mining and agricultural cultivation. However, human activities like mineral resource extraction pose a threat to the ecological environment. To address the conflict between local economic growth and environmental protection, Lvliang City was chosen as the study area to optimize a land use pattern that considers both economic advancement and ecological preservation.

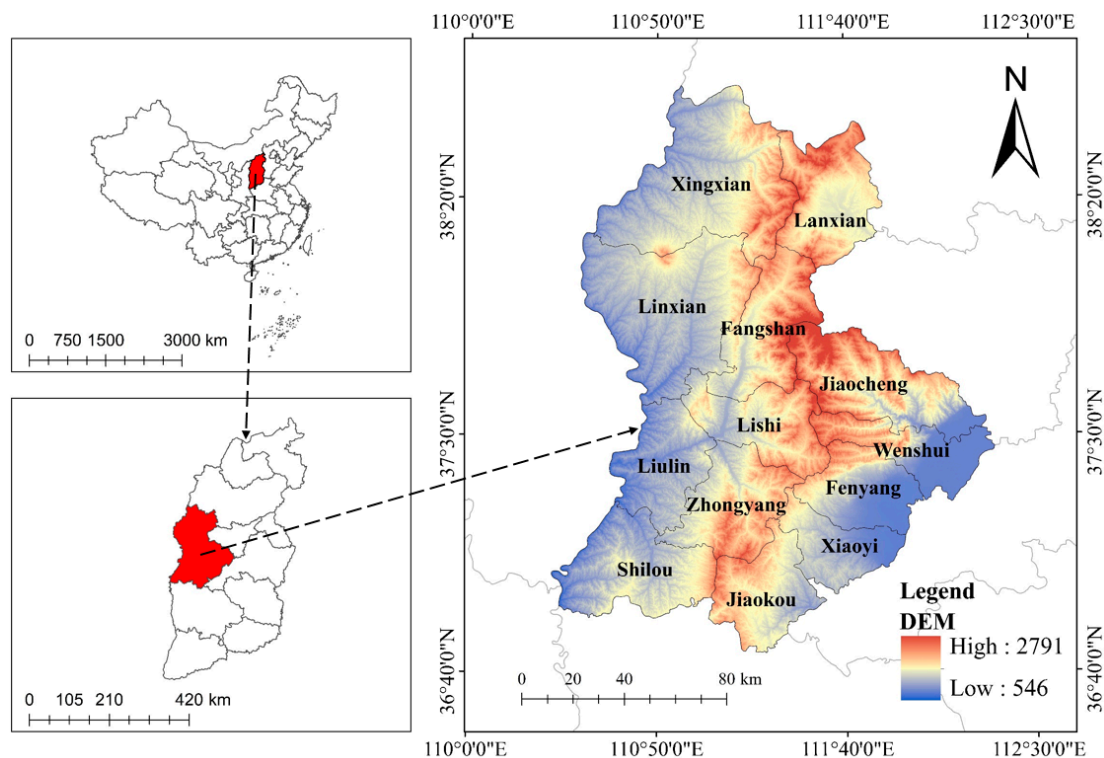


**Figure 1.** Map of the study area.

*2.2. Data Sources*

The data utilized in the study primarily consisted of spatial and textual information. Spatial data includes land use, topographical, and meteorological datasets, while textual data encompasses the Lvliang Statistical Yearbook (2017–2023) and the Land Spatial Planning (2021–2035) datasets. Based on the relevant classification criteria, the present land use data were classified into six main categories. Processing of the spatial data is conducted using the ArcGIS 10.8 platform, with further details provided in Table 1. The data employed in this study were sourced from reputable websites. Extensive research carried out by numerous scholars utilizing these datasets has confirmed their scientific rigor and objectivity, establishing their relevance for investigations into land use optimization.

**Table 1.** Data sources and description.

Data Type	Data Content	Data Description	Data Source
Land Use Type	Land use monitoring data for Lvliang City, 2005, 2010 and 2020	The spatial resolution is 30 m × 30 m, and it was divided into six categories according to the purpose of the study	<a href="https://www.resdc.cn/">https://www.resdc.cn/</a> , accessed on 16 March 2024.
Topographic Data	Soil Type	Image element size is 1000 × 1000	<a href="https://www.resdc.cn/">https://www.resdc.cn/</a> , accessed on 16 March 2024.
	DEM	Initial resolution of 250 m × 250 m	<a href="https://www.resdc.cn/">https://www.resdc.cn/</a> , accessed on 16 March 2024.
	Slope	Initial resolution of 250 m × 250 m	Generated by DEM
	River Data	vector data	<a href="https://www.webmap.cn/">https://www.webmap.cn/</a> , accessed on 16 March 2024.
Meteorological Data	Rainfall Data	Image element size is 1000 × 1000	<a href="https://www.resdc.cn/">https://www.resdc.cn/</a> , accessed on 16 March 2024.
	Temperature Data	Image element size is 1000 × 1000	<a href="https://www.resdc.cn/">https://www.resdc.cn/</a> , accessed on 16 March 2024.

Table 1. Cont.

Data Type	Data Content	Data Description	Data Source
Social Data	GDP	Image element size is 1000 × 1000	<a href="https://www.resdc.cn/">https://www.resdc.cn/</a> , accessed on 16 March 2024.
	Population	Image element size is 1000 × 1000	<a href="https://www.resdc.cn/">https://www.resdc.cn/</a> , accessed on 16 March 2024.
	County Government Locations	Image element size is 1000 × 1000	<a href="https://www.resdc.cn/">https://www.resdc.cn/</a> , accessed on 16 March 2024.
	Primary roads Secondary roads Tertiary roads	Road vector data	<a href="https://www.webmap.cn/">https://www.webmap.cn/</a> , accessed on 16 March 2024.

### 3. Design Framework and Methodology

#### 3.1. Data Processing

##### 3.1.1. Research Framework

The research methodology presented in this paper included three main components (Figure 2):

- (1) **Prediction of Land Use Quantity Structure:** The prediction of land quantity structure involves forecasting the proportions of different land types within a specific area in the future. Four different development scenarios are initially set, as follows: a natural development scenario (NDS), an economic development scenario (EDS), an ecological protection scenario (EPS), and a coordinated development scenario (CDS). The prediction of land use structure under the NDS is based on the land use data of Lvliang City from 2005 and 2020. Using the Markov Chain model, the land area for each type of land use in Lvliang City in 2035 is predicted. This process is implemented in the PLUS model. The EDS and EPS fall under single-objective planning problems, as each of these scenarios requires maximizing either economic or ecological benefits as the sole objective. By calculating and predicting the economic and ecological benefit coefficients for each land type in 2035 and setting constraints for each type of land use, the solution is achieved using LINGO20.0 software. LINGO, developed by Lindo System, Inc. (Chicago, IL, USA) in the United States, is an interactive solver for both linear and general optimization. It effectively addresses nonlinear programming challenges in addition to solving various linear and nonlinear equations, making it a highly versatile tool and an optimal choice for tackling complex optimization models. The CDS falls under multi-objective planning problems, solved using the NSGA-II.
- (2) **Simulation of Land Use Structure Layout:** Based on the predicted land use quantity structures under different scenarios, and using the 2020 land use data as the baseline, the spatial layout of land use in Lvliang City under various future development scenarios is simulated.
- (3) **Analysis of Land Use Layout:** Based on the predicted areas of each land type under different scenarios, the benefits of land use are calculated using ecological and economic benefit coefficients. The ESV is calculated using the Xie Gaodi equivalent factor method. In this study, four landscape pattern indices are selected to analyze the land use layout under different scenarios. These indices include the aggregation index (AI), the largest patch index (LPI), the landscape division index (DIVISION), and the Shannon Diversity Index (SHDI), all calculated using Fragstats4.2 software. These landscape pattern indices reflect the aggregation and dispersion states of the landscape under different development scenarios. Additionally, a land use benefit conversion index is constructed to analyze the efficiency of conversion between ESV and land use benefits. Finally, a comprehensive analysis of land use benefits, ESV, landscape pattern indices, and land use benefit conversion indices under different scenarios is conducted to determine the optimal land use structure.

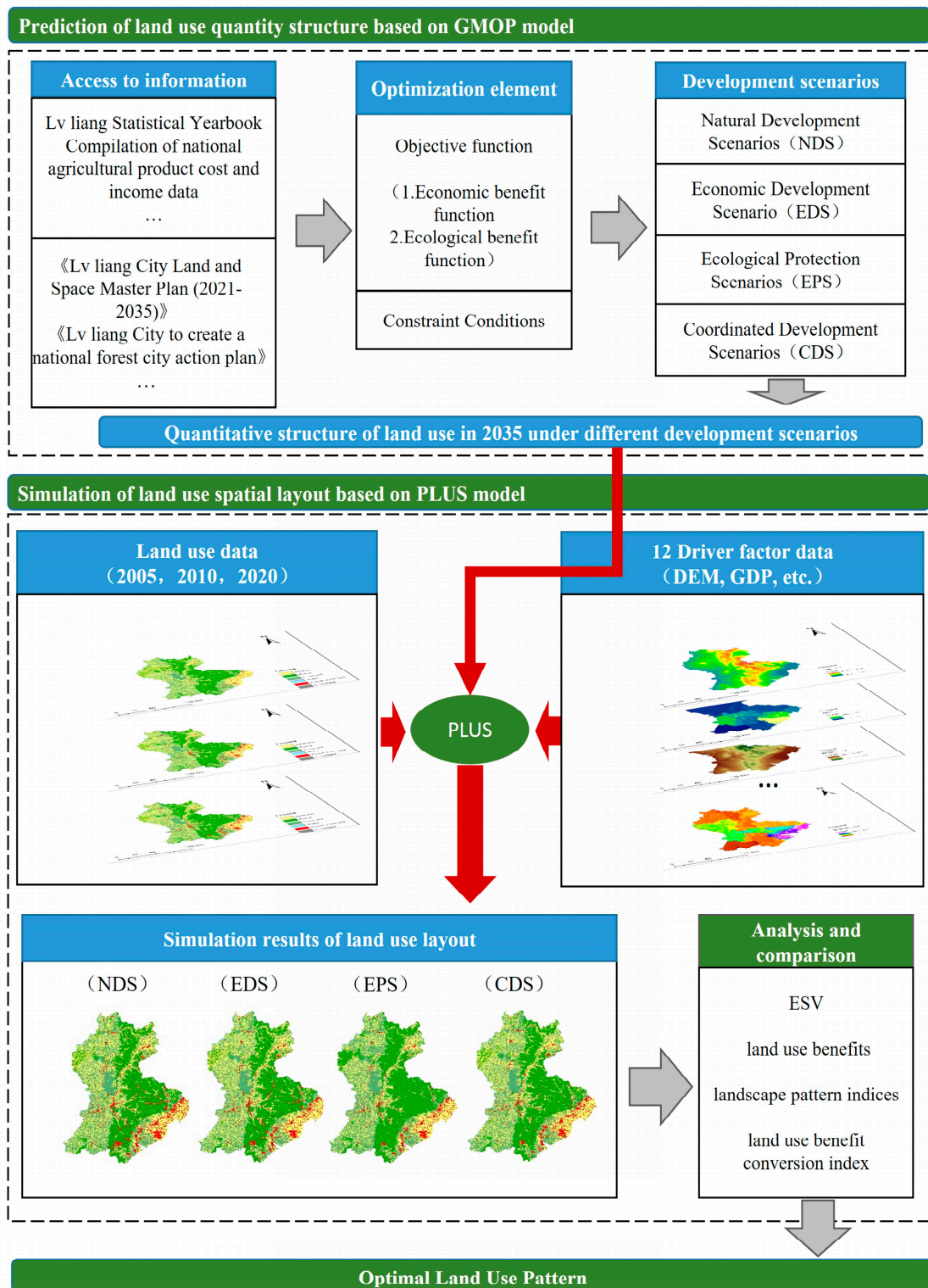
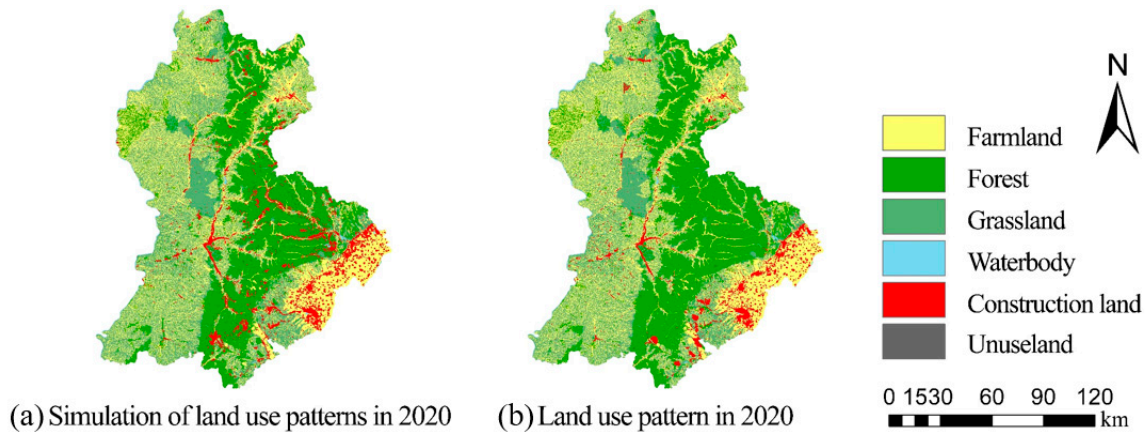


Figure 2. Diagram of the research idea.

### 3.1.2. Verification of Simulation Accuracy

The spatial distribution of land use in Lvliang City in 2020 was obtained by simulating land use data from 2010 (Figure 3). The analysis indicated a strong correspondence between the land use pattern simulated for 2020 by the PLUS model and the actual land use conditions. The arrangement of the six simulated land use categories demonstrated significant agreement with real-world observations. The model's accuracy was evaluated

by comparing the simulated outcomes with the actual 2020 land use data, resulting in a Kappa coefficient of 0.88 and an overall accuracy of 91.60%. These findings underscore the high precision of the PLUS model, confirming its effectiveness in forecasting future land use changes within the study area.



**Figure 3.** Comparison of land use modeling with actual data for 2020.

### 3.2. Methodology

#### 3.2.1. The GMOP Model

The GMOP model is developed by integrating the GM (1, 1) model with the MOP model. Within this framework, the GM model predicts the eco-efficiency and economic coefficients of potential land use types, thereby establishing a foundation for the formulation of the objective function. Meanwhile, the MOP model addresses multi-objective optimization challenges across different scenarios [30], yielding the area allocated to each land use type by the year 2035 under various conditions. The MOP model, a pivotal model in the study of land use optimization, is predicated on constrained data and objective laws to facilitate scientifically grounded predictions. It provides a method for optimizing one or multiple objectives [31]. The detailed model is delineated below:

$$F_1(x) = \max \sum_{j=1}^n a_j x_j \tag{1}$$

$$F_2(x) = \max \sum_{j=1}^n b_j x_j \tag{2}$$

$$s.t = \begin{cases} \sum_{j=1}^n c_{ij} x_j = (\geq, \leq) d_i \quad (i = 1, 2, 3 \dots, m) \\ x_j \geq 0 \quad (j = 1, 2, 3 \dots, n) \end{cases} \tag{3}$$

where  $F_1(x)$  and  $F_2(x)$  denote the functions for land economic benefits and ecological benefits, respectively. Here,  $x_j$  represents the area allocated to each land use type, while  $n$  indicates the total number of variables. The coefficients  $a_j$  and  $b_j$  relate to the economic and ecological benefit coefficients for each respective land use type. The notation “s.t” indicates the constraints imposed on land use for each category, with  $c_{ij}$  representing the coefficient associated with the  $j$ -th variable in the  $i$ -th constraint, and  $m$  signifying the total number of constraint conditions. Finally,  $d_i$  pertains to the  $i$ -th constraint condition.

#### 3.2.2. The PLUS Model

The PLUS model, operating as a grid-based cellular automaton (CA), is used to simulate land use and land cover (LULC) changes. This model integrates a land expansion analysis strategy (LEAS) within the CA framework, enabling the exploration of different

land use transitions. It supports the creation of various scenarios to forecast and analyze future land use dynamics [32].

- (1) **Adaptation Probability.** The LEAS module incorporates a stochastic sampling mechanism designed to reduce computational costs while simultaneously utilizing the random forest algorithm to assess the development probabilities associated with various land use types. The formula is presented as follows:

$$P_{i,k(X)}^d = \frac{\sum_{n=1}^M I[hn(X) = d]}{M} \quad (4)$$

where  $M$  denotes the total count of decision trees,  $X$  represents the vector that comprises the driving factors,  $hn(X)$  indicates the predicted land use type generated by the  $n$ -th decision tree, and  $d$  takes on a value of either 0 or 1.

- (2) **Adaptive Inertia Coefficient.** This coefficient is adaptively adjusted during repeated runs, based on the discrepancy between the expected land type data and the actual land type data. This mechanism effectively mitigates the uncertainties and complexities associated with natural processes and human activities involved in land use conversion. Consequently, it improves the accuracy of the simulation model and attains the intended outcomes regarding land use types [33]. The formula is as follows:

$$D_k^t = \begin{cases} D_k^{t-1} (|G_k^{t-1}| \leq |G_k^{t-2}|) \\ D_k^{t-1} \times \frac{G_k^{t-2}}{G_k^{t-1}} (0 > G_k^{t-2} > G_k^{t-1}) \\ G_k^{t-1} \times \frac{G_k^{t-1}}{G_k^{t-2}} (G_k^{t-1} > G_k^{t-2} > 0) \end{cases} \quad (5)$$

where  $D_k^t$  signifies the inertia coefficient for the  $k$ -th land use type at time  $t$ . Additionally,  $G_k^{t-1}$  and  $G_k^{t-2}$  represent the discrepancies between the actual land amount and the demand at times  $t - 1$  and  $t - 2$ , respectively.

- (3) **Optimization of Land Use Layout.** Twelve factors, encompassing elevation, slope, population, soil type, GDP, road networks, rivers, and distance to the county government seat, are identified as driving forces for land use change. Concurrently, water bodies are designated as restricted areas during the optimization process. The precision of the model is assessed through two primary parameters: overall accuracy and the Kappa coefficient.

### 3.2.3. Constructing the Objective Function

- (1) **Economic Benefit Function.** The economic advantages of land are primarily defined by the economic output per unit area for each category of land. This study utilizes statistical yearbooks from Luliang City spanning the years 2017 to 2023. The output for cultivated and forest land is indicated by the values of agricultural and forestry production, respectively. The output for grassland is denoted by the value derived from animal husbandry, while the output for aquatic areas is represented by the fishery output value. Furthermore, the economic impact of construction land is demonstrated through the output values generated by the secondary and tertiary industries.
- (2) **Ecological Benefit Function.** The ecological benefit coefficients of land are primarily assessed using the equivalent factor method, as suggested by researchers such as Xie Gaodi. This methodology primarily captures the ESV provided by land. Since the supply services of land ecosystems are already incorporated into the economic benefits, the ecological advantages encompass the regulatory, supporting, and cultural services of ecosystems. This study employs the terrestrial ESV equivalent factor method, as recommended by scholars, including Xie Gaodi [34], for the purpose of evaluation. Additionally, the equivalent factor table is adjusted based on the ratio of



the NPP level in Lvliang City compared to the national average [35]. Data regarding the prices of local food crops and their yield per unit area are obtained by consulting the Lvliang Statistical Yearbook from 2016 to 2022. The ESV is quantified at one-seventh of the economic value linked to grain production per unit area of farmland. This value encompasses a range of ecosystem services, including supply, regulatory, supporting, and cultural services. Acknowledging that supply services are included within economic benefits, ecological benefits are delineated by regulatory, supporting, and cultural services. Annual coefficients for land ecological benefits are calculated, and these coefficients are projected for Lvliang City in 2035 using the GM (1: 1) model. To ensure the reliability of the revised eco-efficiency coefficients for land, a sensitivity index is employed to evaluate how variations in these coefficients affect the total ESV for each land type. The sensitivity of ESV to these coefficients is evaluated by modifying the eco-efficiency coefficients for each land type by  $\pm 50$  percent. The formula is as follows:

$$C_s = \frac{(E_2 - E_1)/E_1}{(V_{2i} - V_{1i})/V_{1i}} \quad (6)$$

where  $C_s$  denotes the sensitivity index that measures the response of a specific land type to the value of land ecosystem services.  $E_1$  and  $E_2$  represent the ESV in Lvliang City prior to and following the adjustment, respectively.  $V_{1i}$  and  $V_{2i}$  indicate the ecological benefit coefficients for the  $i$ -th land type before and after the adjustment, respectively. A  $C_s$  value of less than 1 indicates that the ESV is inelastic regarding the ecological benefit coefficients of that land type. Lower  $C_s$  values suggest a diminished responsiveness of the assessment of land ESV to the precision of the ecological benefit coefficients, thereby indicating a higher degree of rationality in the coefficients [36]. Relevant parameters are shown in Tables 2 and 3.

**Table 2.** Parameters of economic and ecological benefits per unit area of land use type (unit: RMB/km<sup>2</sup>).

Efficiency	Farmland	Forest	Grassland	Waterbody	Construction Land	Unused Land
economic efficiency	808.48	167.74	247.83	44.76	164,272.42	0.01
eco-efficiency	33.88	215.17	92.42	1316.57	0	2.47

**Table 3.** Sensitivity coefficients for each land use type.

Year	Farmland	Forest	Grassland	Waterbody	Construction Land	Unused Land
2005	0.0043	0.0268	0.0096	0.0036	0	0.0001
2020	0.0015	0.0093	0.0037	0.0011	0	0.0001

#### 3.2.4. Restrictive Condition

The constraints are primarily established in accordance with a series of land use policies and regulations promulgated by Lvliang City and Shanxi Province, including but not limited to “The Overall Planning of Lvliang City’s Territorial Space (2021–2035)”, the State Council’s approval of “The Territorial Spatial Planning of Shanxi Province (2021–2035),” and “The Action Plan for Lvliang City to Create a National Forest City”. These constraints delineate a series of conditions for socio-economic development and ecological protection, as specified in Table 4.

**Table 4.** Constraint information.

Constraint	Prerequisite	Foundation
Total land area	$X_1 + X_2 + X_3 + X_4 + X_5 + X_6 = 21,115.57 \text{ km}^2$	Total land area constraint.
Farmland	$4165.34 \text{ km}^2 \leq X_1 \leq X_1^+$ , $X_1^+$ is the area of farmland in Lvliang City in 2020	The Lvliang City Territorial Spatial Master Plan (2021–2035) calls for farmland holdings of 4165.342 km <sup>2</sup> .
Forest	$6334.67 \text{ km}^2 \leq X_2 \leq 7528.98 \text{ km}^2$	Action Programme for the Creation of a National Forest City in Lvliang City: Lvliang citywide forest cover of more than 30 per cent, which is less than 1.1 times the current value in 2020.
Grassland	$6453.09 \text{ km}^2 \leq X_3 \leq 6906.55 \text{ km}^2$	Greater than projected under natural development conditions and less than 1.1 times the current value in 2020.
Waterbody	$121.17 \text{ km}^2 \leq X_4 \leq 129.76 \text{ km}^2$	Greater than the current value in 2020 and less than the projected value of natural development.
Construction land	$898.41 \text{ km}^2 \leq X_5 \leq 1167.94 \text{ km}^2$	The State Council’s approval of the “Shanxi Province Land Space Planning (2021–2035)” requires that the expansion of the urban development boundary be controlled within 1.3 times the size of the urban construction land based on 2020, with 1.3 times the existing construction land in Lvliang City as the upper boundary, and the lower boundary as the status quo value in 2020.
Unused Land	$0.37 \text{ km}^2 \leq X_6 \leq 0.52 \text{ km}^2$	Greater than the current value in 2020 and less than the projected value of natural development.

**4. Results**

*4.1. Analysis of the Quantitative Structure of Land Use*

According to the statistical data presented in Table 5, the NDS indicated a substantial increase in built-up land, which rose by 55.05% compared to 2020. Furthermore, grassland, water bodies, and unused land experienced increases of 27.78%, 7.09%, and 39.13%, respectively. In contrast, farmland and forest land decreased by 4.39% and 5.43%, respectively, compared to 2020. The NDS encompassed land use changes from 2005 to 2020, which were used to predict the areas of various land types in 2035. During this period, the areas of farmland and forest land decreased, while the areas of built-up land, grassland, water bodies, and unused land increased. Consequently, the anticipated changes in land areas by 2035 reflected the trends observed between 2005 and 2020. In this context, the unrestricted expansion of built-up land encroached upon both farmland and forest land, highlighting a distinctly unreasonable land use strategy.

**Table 5.** Changes in land quantity structure under different development scenarios (unit: km<sup>2</sup>).

Land Type	2020	Development Scenarios			
		Natural Development	Economic Development	Ecological Protection	Coordinated Development
Farmland	6972.40	6666.23	6972.40	5651.49	6724.29
Forest	6844.53	6473.01	6334.67	7528.98	6664.74
Grassland	6278.68	6453.08	6519.02	6906.55	6581.84
Waterbody	121.17	129.76	121.17	129.76	126.94
Construction land	898.41	1392.96	1167.94	898.41	1017.33
Unused Land	0.37	0.52	0.37	0.37	0.42

In the EDS, forest land experienced a notable reduction, declining by 7.45% relative to 2020. Areas set aside for cropland, water bodies and unused land remain unchanged. In contrast, grassland saw an increase of 3.83%, while construction land expanded significantly by 30%. Construction land is a vital component supporting economic development, hence the substantial increase. Lvliang City’s agricultural economy is well-developed, so under the EDS, efforts were made to maintain farmland. Additionally, a slight increase in grassland area was observed, attributed to the high output value of animal husbandry in Lvliang City. In this development scenario, although the growth of built-up land slowed, it continued to increase at an unsustainable rate. The area of farmland did not exhibit

a significant decrease; however, the area of forest land declined markedly, which posed serious challenges to ecological protection efforts.

In the EPS, the farmland area underwent a significant decrease of 18.95% compared to 2020. In contrast, both forest land and grassland increased by 10% relative to the same year. The areas designated for construction land and unused land remained stable, while water bodies experienced an increase of 7.09%. As demonstrated in Table 2, forest land and water bodies were associated with greater ecological benefits. Consequently, under the EDS, these areas were expanded, while construction land and unused land, which have low ecological benefits, were maintained at their existing levels. In comparison to economic benefits, the ecological benefits of farmland are negligible, leading to its substantial reduction. In this scenario, although the expansion of built-up land area was minimal, substantial increases were noted in both forest and grassland areas. Conversely, the cultivated land area faced a notable decline. Considering the importance of construction and agricultural lands for the economic development of Lvliang City, this development scenario, although advantageous for ecological preservation, was evidently insufficient to support the local economy.

In the CDS, both farmland and forest land areas underwent slight reductions, decreasing by 3.69% and 2.70%, respectively, relative to 2020. Conversely, grassland and water body areas demonstrated increases of 4.61% and 4.55%, respectively. The area allocated for construction experienced a significant growth of 11.69%, whereas the extent of unused land expanded by 12.54%. When compared to the EDS, the increase in construction land was more modest, and the areas of grassland and water bodies saw modest increases. In comparison to the EPS, the decrease in farmland was less substantial, and the change in forest land area was minimal. Consequently, the land use pattern established in this development scenario effectively addressed the requirements for economic growth while also reducing the conflict between economic development and ecological preservation.

#### 4.2. Simulation Analysis of Spatial Layout of Land Use Structure

The land-use pattern simulation of the four scenarios is shown in Figure 4. In the NDS, a significant increase in construction land was observed, primarily reflecting an outward expansion from the city center in all directions. The most pronounced growth occurred in the southern region, where forested areas and farmland were notably reduced to accommodate this expansion. Additionally, the southeastern sector experienced considerable growth in construction land, mainly resulting from the encroachment upon farmland. Significant reductions were observed in both forest and farmland areas, whereas the grassland area experienced an increase, predominantly concentrated in the northern region, characterized by the encroachment on forest land.

In the EDS, a rapid expansion of construction land was observed, predominantly characterized by an outward extension from the city center in all directions. The southern region of Lvliang City experienced particularly significant growth in construction land, largely at the expense of forested areas. Conversely, the southeastern region did not exhibit notable changes in construction land, as it was primarily composed of farmland, which remained stable under this scenario. Consequently, no substantial expansion of construction land occurred in that area. Additionally, an increase in grassland was documented, especially in the central-western and western regions, with the latter showing a more pronounced growth, largely due to encroachment on forested land.

In the EPS, notable increases were recorded in both forest and grassland areas. The northwestern region experienced substantial expansion of forest land, which was characterized by diffusion in various directions. Similarly, the central-eastern area also saw a rise in forest land, primarily due to encroachment upon farmland. Grassland expansion was predominantly concentrated in the northwest, largely at the expense of agricultural fields. Overall, the area of farmland diminished significantly, with major reductions documented in the northwest and central-eastern regions, attributed to the encroachment of both forest and grassland. In contrast, the southeastern region did not display significant contraction

in farmland. Additionally, the area designated for construction remained stable, while the water body area increased.

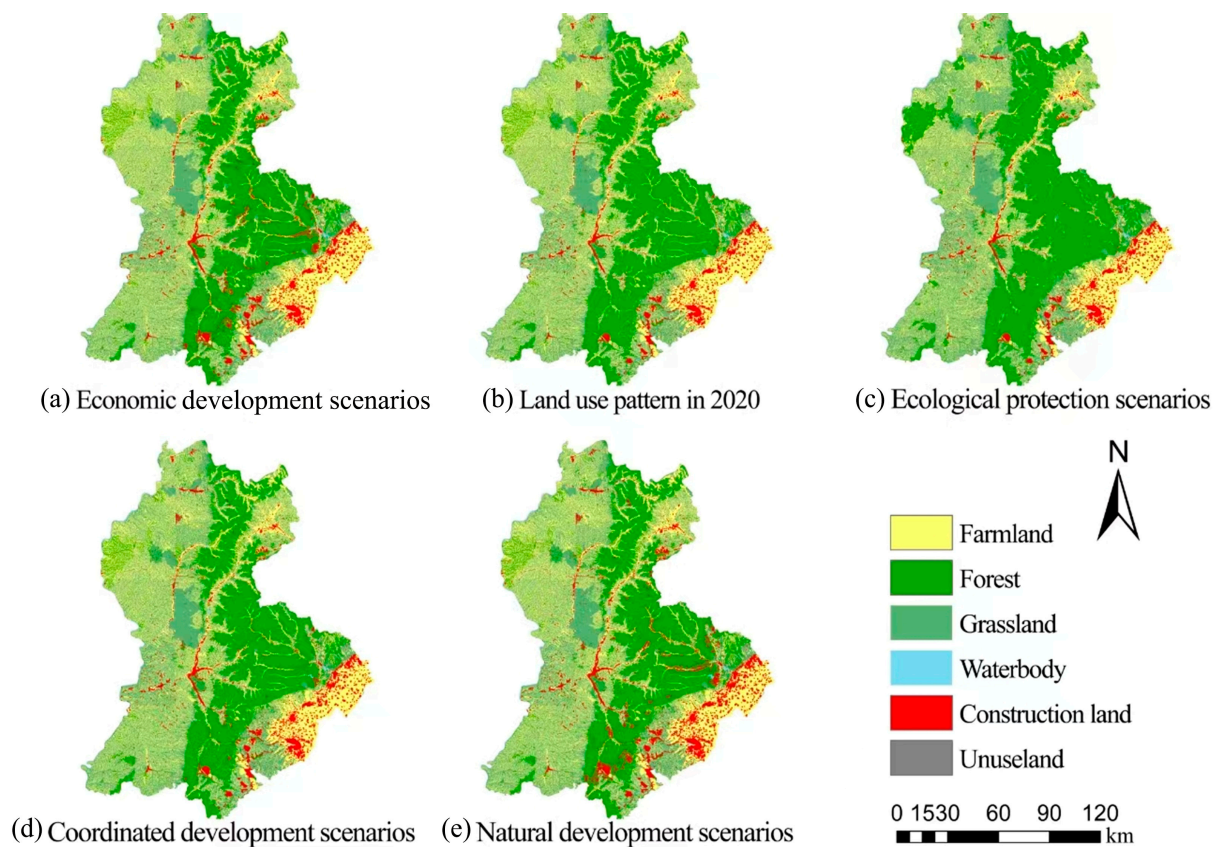


**Figure 4.** Land use simulation of Lvliang City under different development scenarios in 2035.

In the CDS, an expansion of construction land was observed, predominantly marked by the urban area's extension in multiple directions. In the southern region, although construction land expanded, the pace of growth was relatively gradual. Importantly, there were no substantial decreases in the areas designated for arable or forest land. Conversely, an increase in grassland was noted in both the central and northern regions.

Figure 5 indicates that the EPS demonstrated the highest LPI, whereas the EDS recorded the lowest LPI. Generally, a higher LPI indicates the presence of a greater number of large patches in the landscape, with less human disturbance to natural landscapes. The LPI for the CDS was more like that of 2020 and exceeded the values observed in both the NDS and EDS. This finding suggests that the landscape in the CDS experienced less impact from human activities than that in the EDS. This result indicated a greater degree of landscape patch aggregation in the CDS relative to the EPS. With regard to the SHDI, the NDS demonstrated the highest value. In contrast, the CDS was found to be comparable to both the EDS and the land use pattern of 2020, while surpassing the EPS. This finding indicated that the CDS supported greater species diversity. Regarding the DIVISION, no notable differences were observed across the various development scenarios. Overall, in the CDS, the land use pattern was characterized by lower levels of human disturbance. The landscape patches were more cohesively clustered, biodiversity was richer, and the quality of the ecological environment was higher.

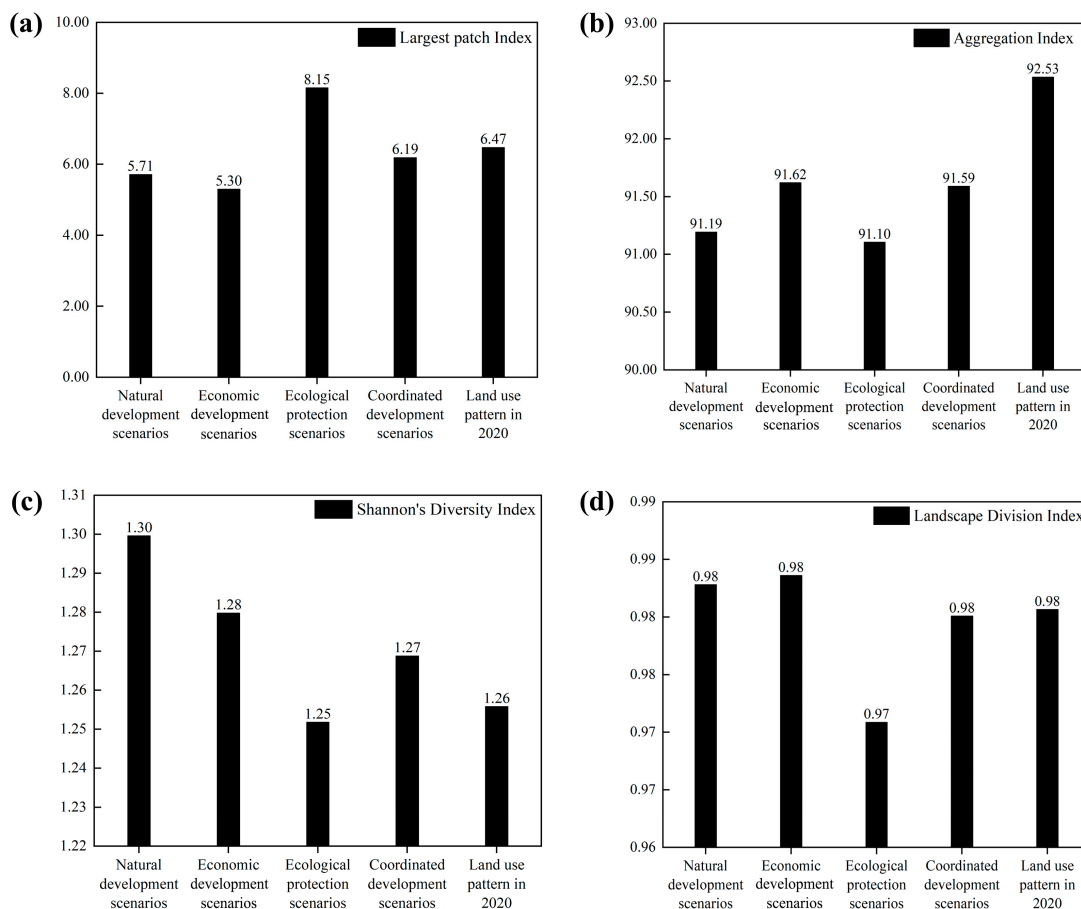


**Figure 5.** Landscape index for different development scenarios in Lvliang, 2035. (a) Largest patch index; (b) Aggregation index; (c) Shannon Diversity Index; (d) Landscape division index.

### 4.3. Land Use Benefits and ESV

Using the projected economic and ecological benefit coefficients for land use in Lvliang City in 2035, as detailed in prior sections, the benefits of land use across different development scenarios for that year are calculated. The ESV equivalents from the years 2016 to 2022 were applied, and the GM (1: 1) model was used to predict the ESV equivalents for Lvliang City in 2035. These predictions, along with the updated equivalent factor table, facilitated the calculation of ESV for the simulated land use patterns across different scenarios in 2035.

As indicated in Table 6, the NDS yielded the highest land use benefits; however, the corresponding ESV were comparatively low. In contrast, the EDS demonstrated increased land use benefits but recorded the lowest ESV. Conversely, the EPS achieved the highest ESV, albeit with the lowest land use benefits. This outcome, while satisfying ecological protection standards, proved detrimental to economic development. The CDS demonstrated both high land use benefits and high ESV, capable of balancing economic growth with environmental quality.

**Table 6.** Land use benefits and ESV under different scenarios in 2035 (Unit: million yuan).

Development Scenario	Land Use Benefits	Ecosystem Services Values
Natural Development Scenario	23,929.02	263.08
Economic Development Scenario	20,254.13	260.87
Ecological Protection Scenarios	15,775.43	286.65
Coordinated Development Scenario	17,553.64	268.61
2020 Land Use Pattern	15,837.95	270.14

Numerous studies indicate that changes in land use patterns within a region significantly affect ESV and land use benefits [37,38]. Improvements and optimizations in land use enhance the capacity for ecosystem services. However, during the transition of land use patterns, economic development and ecological protection within a region often appear mutually exclusive, with economic development frequently occurring at the expense of the environment. To examine the economic benefits that can be obtained at the cost of ecological benefits, this study uses land use benefits to represent economic benefits and ESV to represent ecological benefits. An index for land use benefit conversion ( $I$ ) is established to explore the conversion efficiency between land use benefits and ESV when land use patterns transition to different scenarios in 2020. A larger index ( $I$ ) indicates that for each unit of ecological benefit sacrificed, greater economic benefits are achieved, suggesting that the transformation of land use patterns in these scenarios has greater developmental potential and is more conducive to sustainable development. The formula is as follows:

$$I = \left| \frac{LUE_2 - LUE_1}{E_4 - E_3} \right| \quad (7)$$

where  $LUE_2$  denotes the land use benefits associated with various development scenarios, while  $LUE_1$  reflects the land use benefits derived from the 2020 land use pattern as projected for 2035. Similarly,  $E_4$  indicates the ESV corresponding to different development scenarios, and  $E_3$  represents the ESV of the 2020 land use pattern projected for 2035.

Figure 6 illustrates that the conversion rate associated with the NDS was the highest. However, this scenario's land use pattern underwent significant expansion of construction land, surpassing the established constraints and failing to align with the future development objectives of Lvliang City. The conversion rate observed in the CDS approached that of the NDS, while it was markedly higher than those recorded for both the EDS and EPS. This indicated that transitioning from the 2020 land use pattern to the pattern under the CDS would yield the highest land use benefits per unit sacrifice of ESV, suggesting a high potential for land development and greater sustainability under this pattern.

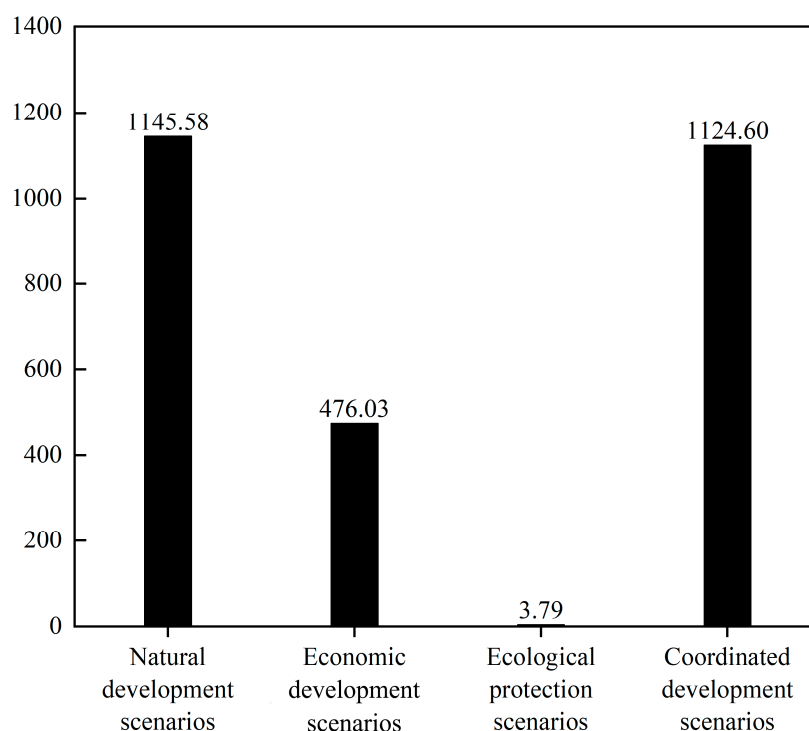


**Figure 6.** Conversion rates of ESV to land use benefits under different development scenarios.

## 5. Discussion

This study used land use data from 2005 and 2020 along with GMOP and PLUS models to simulate both the quantity and spatial distribution of land use, predicting land use patterns for 2035 under various development scenarios. Previous research primarily identified optimal land use patterns by analyzing ecosystem service value (ESV) and land use benefits across different development scenarios [39,40]. However, these studies did not account for the conversion efficiency between ESV and land use benefits during the transition from the current land use pattern to future scenarios, nor did they consider the impact of land use pattern changes on landscape configurations [41]. Consequently, this study introduced a land use benefit conversion index to represent the conversion efficiency between ESV and land use benefits for the first time. A comprehensive analysis of ESV, land use benefits, landscape pattern indices, and the land use benefit conversion index was performed to evaluate these indicators and identify the optimal land use pattern. The research findings provide scientific theoretical support for land use optimization and ecological protection in Lvliang City and offer a methodological example for land use optimization in other regions.

However, the study has some limitations. The land use categories were divided into six primary categories, which, while reflecting changes in various land types under different scenarios in Lvliang City, do not fully explain the relationship between economic development, ecological protection, and mining development in a city rich in mineral resources. The construction land category should be further detailed into types such as mining land to explore its relationship with the economy and ecology. The ESV in this study was calculated based on the equivalent factor table by Xie Gaudi. Although the equivalent factors are simple, widely applicable, and have low data requirements [42], they have certain limitations in accuracy, dynamism, complexity, and regional applicability. A more in-depth analysis combined with other methods is needed to improve the comprehensiveness and accuracy of the assessment.

Given the limitations of this study, future research should develop a more targeted land use classification system and conduct a thorough analysis of the relationships among economic development, ecological protection, and mining activities in mineral resource-based cities. Additionally, the objective and comprehensive assessment of ESV within a region, along with the reduction of errors introduced by subjective factors, necessitates further exploration and analysis in future studies to improve the accuracy and objectivity of the evaluation results.

## 6. Conclusions

In this study, a multi-objective structural optimization model that integrates GMOP and PLUS was developed to achieve a balance among the economic, social, and ecological benefits of land use. Various scenarios regarding land use structures were derived for different development contexts in Lvliang City, based on specific constraints. The key findings of this research are summarized as follows:

- (1) The GMOP and PLUS coupling models are used to determine land use structure and spatial distribution under various development objectives. By employing this coupled approach, land use patterns for Lvliang City are derived across four distinct development scenarios.
- (2) From the perspective of landscape patterns, the land use pattern under the CDS is characterized by minimal human disturbance, enhanced patch aggregation, greater species diversity, and improved ecological quality.
- (3) The land use benefits under the NDS, EDS, EPS, and CDS are 2392.902 billion yuan, 2025.413 billion yuan, 1577.543 billion yuan, and 1755.364 billion yuan, respectively. The ESV are 26.308 billion yuan, 26.087 billion yuan, 28.665 billion yuan, and 26.861 billion yuan, respectively. This shows that the CDS can meet economic development needs while also considering ecological environment protection.

- (4) Under the CDS, when the areas of cultivated land, grassland, forest land, water bodies, construction land, and unused land are 6724.29 km<sup>2</sup>, 6664.74 km<sup>2</sup>, 6581.84 km<sup>2</sup>, 126.94 km<sup>2</sup>, 1017.33 km<sup>2</sup>, and 0.42 km<sup>2</sup>, respectively, the land use benefit conversion index is at its highest.

The research method outlined in this paper provides a valuable reference for optimizing urban land use structures. The findings establish a foundation for developing land use planning and management policies in resource-based cities.

**Author Contributions:** Conceptualization, methodology, writing—review and editing, and supervision, Z.W. and A.Z.; methodology, software, visualization, and writing—original draft preparation, A.Z.; investigation and validation, Z.W.; supervision, Q.L. All authors have read and agreed to the published version of the manuscript.

**Funding:** This research was funded by the Key R&D project for school local cooperation in Lvliang City, grant number 2022XDHZ12.

**Institutional Review Board Statement:** Not applicable.

**Informed Consent Statement:** Not applicable.

**Data Availability Statement:** The data presented in this study are available on request from the corresponding author. The data are not publicly available due to privacy restrictions.

**Conflicts of Interest:** The authors declare no conflicts of interest.

## References

- Zhao, X.; Pu, J.; Wang, X.; Chen, J.; Yang, L.E.; Gu, Z. Land-Use Spatio-Temporal Change and Its Driving Factors in an Artificial Forest Area in Southwest China. *Sustainability* **2018**, *10*, 4066. [\[CrossRef\]](#)
- Rimal, B.; Zhang, L.; Keshtkar, H.; Wang, N.; Lin, Y. Monitoring and Modeling of Spatiotemporal Urban Expansion and Land-Use/Land-Cover Change Using Integrated Markov Chain Cellular Automata Model. *ISPRS Int. J. Geo-Inf.* **2017**, *6*, 288. [\[CrossRef\]](#)
- Zscheischler, J.; Rogga, S.; Lange, A. The success of transdisciplinary research for sustainable land use: Individual perceptions and assessments. *Sustain. Sci.* **2018**, *13*, 1061–1074. [\[CrossRef\]](#)
- Zhang, H.B.; Zhang, X.H. Land use structural optimization of Lilin based on GMOP-ESV. *Trans. Nonferrous Met. Soc. China* **2011**, *21*, S738–S742. [\[CrossRef\]](#)
- Chuai, X.W.; Huang, X.J.; Wu, C.Y.; Li, J.B.; Lu, Q.L.; Qi, X.X.; Zhang, M.; Zuo, T.H.; Lu, J.Y. Land use and ecosystems services value changes and ecological land management in coastal Jiangsu, China. *Habitat Int.* **2016**, *57*, 164–174. [\[CrossRef\]](#)
- MohanRajan, S.N.; Loganathan, A.; Manoharan, P. Survey on Land Use/Land Cover (LULC) change analysis in remote sensing and GIS environment: Techniques and Challenges. *Environ. Sci. Pollut. Res.* **2020**, *27*, 29900–29926. [\[CrossRef\]](#)
- Torres, P.; Rodes-Blanco, M.; Viana-Soto, A.; Nieto, H.; García, M. The Role of Remote Sensing for the Assessment and Monitoring of Forest Health: A Systematic Evidence Synthesis. *Forests* **2021**, *12*, 1134. [\[CrossRef\]](#)
- Liu, H.; Wang, Y.; Sang, L.L.; Zhao, C.S.; Hu, T.Y.; Liu, H.T.; Zhang, Z.; Wang, S.Y.; Miao, S.X.; Ju, Z.S. Evaluation of Spatiotemporal Changes in Cropland Quantity and Quality with Multi-Source Remote Sensing. *Land* **2023**, *12*, 1764. [\[CrossRef\]](#)
- Ma, Q.Q.; Chai, L.R.; Hou, F.J.; Chang, S.H.; Ma, Y.S.; Tsunekawa, A.; Cheng, Y.X. Quantifying Grazing Intensity Using Remote Sensing in Alpine Meadows on Qinghai-Tibetan Plateau. *Sustainability* **2019**, *11*, 417. [\[CrossRef\]](#)
- Zhong, A.Y.; Hu, C.M.; You, L. Evaluation and Prediction of Ecological Restoration Effect of Beijing Wangping Coal Mine Based on Modified Remote Sensing Ecological Index. *Land* **2023**, *12*, 2059. [\[CrossRef\]](#)
- Ma, S.H.; Wen, Z.Z. Optimization of land use structure to balance economic benefits and ecosystem services under uncertainties: A case study in Wuhan, China. *J. Clean Prod.* **2021**, *311*, 127537. [\[CrossRef\]](#)
- Wu, R.; Lan, H.F.; Cao, Y.X.; Li, P.Y. Optimization of low-carbon land use in Chengdu based on multi-objective linear programming and the future land use simulation model. *Front. Environ. Sci.* **2022**, *10*, 989747. [\[CrossRef\]](#)
- Zhang, P.; Liu, L.; Yang, L.; Zhao, J.; Li, Y.; Qi, Y.; Ma, X.; Cao, L. Exploring the response of ecosystem service value to land use changes under multiple scenarios coupling a mixed-cell cellular automata model and system dynamics model in Xi'an, China. *Ecol. Indic.* **2023**, *147*, 110009. [\[CrossRef\]](#)
- Shi, Q.; Gu, C.-J.; Xiao, C. Multiple scenarios analysis on land use simulation by coupling socioeconomic and ecological sustainability in Shanghai, China. *Sustain. Cities Soc.* **2023**, *95*, 104578. [\[CrossRef\]](#)
- Huang, Y.; Nian, P.; Zhang, W. The prediction of interregional land use differences in Beijing: A Markov model. *Environ. Earth Sci.* **2014**, *73*, 4077–4090. [\[CrossRef\]](#)



16. Du, Y.; Li, X.; He, X.; Li, X.; Yang, G.; Li, D.; Xu, W.; Qiao, X.; Li, C.; Sui, L. Multi-Scenario Simulation and Trade-Off Analysis of Ecological Service Value in the Manas River Basin Based on Land Use Optimization in China. *Int. J. Environ. Res. Public Health* **2022**, *19*, 6216. [[CrossRef](#)]
17. Zhang, W.; Wang, H.; Han, F.; Gao, J.; Nguyen, T.; Chen, Y.; Huang, B.; Zhan, F.B.; Zhou, L.; Hong, S. Modeling urban growth by the use of a multiobjective optimization approach: Environmental and economic issues for the Yangtze watershed, China. *Environ. Sci. Pollut. Res. Int.* **2014**, *21*, 13027–13042. [[CrossRef](#)]
18. Zhu, L.Z.; Huang, Y.P. Multi-Scenario Simulation of Ecosystem Service Value in Wuhan Metropolitan Area Based on PLUS-GMOP Model. *Sustainability* **2022**, *14*, 13604. [[CrossRef](#)]
19. Li, C.; Wu, Y.M.; Gao, B.P.; Zheng, K.J.; Wu, Y.; Li, C. Multi-scenario simulation of ecosystem service value for optimization of land use in the Sichuan-Yunnan ecological barrier, China. *Ecol. Indic.* **2021**, *132*, 108328. [[CrossRef](#)]
20. Mo, J.X.; Sun, P.L.; Shen, D.D.; Li, N.; Zhang, J.Y.; Wang, K. Simulation Analysis of Land-Use Spatial Conflict in a Geopark Based on the GMOP-Markov-PLUS Model: A Case Study of Yimengshan Geopark, China. *Land* **2023**, *12*, 1291. [[CrossRef](#)]
21. Firozjaei, M.K.; Sedighi, A.; Argany, M.; Jelokhani-Niaraki, M.; Arsanjani, J.J. A geographical direction-based approach for capturing the local variation of urban expansion in the application of CA-Markov model. *Cities* **2019**, *93*, 120–135. [[CrossRef](#)]
22. Verburg, P.H.; Soepboer, W.; Veldkamp, A.; Limpiada, R.; Espaldon, V.; Mastura, S.S.A. Modeling the spatial dynamics of regional land use: The CLUE-S model. *Environ. Manag.* **2002**, *30*, 391–405. [[CrossRef](#)] [[PubMed](#)]
23. Zhang, Y.; Yu, P.H.; Tian, Y.S.; Chen, H.T.; Chen, Y.Y. Exploring the impact of integrated spatial function zones on land use dynamics and ecosystem services tradeoffs based on a future land use simulation (FLUS) model. *Ecol. Indic.* **2023**, *150*, 110246. [[CrossRef](#)]
24. Liang, X.; Guan, Q.F.; Clarke, K.C.; Liu, S.S.; Wang, B.Y.; Yao, Y. Understanding the drivers of sustainable land expansion using a patch-generating land use simulation (PLUS) model: A case study in Wuhan, China. *Comput. Environ. Urban Syst.* **2021**, *85*, 101569. [[CrossRef](#)]
25. Zhong, Y.; Zhang, X.; Yang, Y.; Xue, M. Optimization and Simulation of Mountain City Land Use Based on MOP-PLUS Model: A Case Study of Caijia Cluster, Chongqing. *ISPRS Int. J. Geo-Inf.* **2023**, *12*, 451. [[CrossRef](#)]
26. Shu, R.; Wang, Z.; Guo, N.; Wei, M.; Zou, Y.; Hou, K. Multi-Scenario Land Use Optimization Simulation and Ecosystem Service Value Estimation Based on Fine-Scale Land Survey Data. *Land* **2024**, *13*, 557. [[CrossRef](#)]
27. Luan, C.; Liu, R.; Zhang, Q.; Sun, J.; Liu, J. Multi-objective land use optimization based on integrated NSGA-II-PLUS model: Comprehensive consideration of economic development and ecosystem services value enhancement. *J. Clean Prod.* **2024**, *434*, 140306. [[CrossRef](#)]
28. Meng, F.; Zhou, Z.; Zhang, P. Multi-Objective Optimization of Land Use in the Beijing-Tianjin-Hebei Region of China Based on the GMOP-PLUS Coupling Model. *Sustainability* **2023**, *15*, 3977. [[CrossRef](#)]
29. Chen, N.; Xin, C.L.; Tang, D.B.; Zhang, L.; Xin, S.J. Multi-scenario land use optimization and carbon stock assessment in Northwest China. *Chin. J. Environ. Sci.* **2023**, *44*, 4655–4665.
30. Guo, P.F.; Wang, H.Y.; Qin, F.; Miao, C.H.; Zhang, F.F. Coupled MOP and PLUS-SA Model Research on Land Use Scenario Simulations in Zhengzhou Metropolitan Area, Central China. *Remote Sens.* **2023**, *15*, 3762. [[CrossRef](#)]
31. Wang, Z.M.; Guo, M.D.; Zhang, D.; Chen, R.Q.; Xi, C.F.; Yang, H.B. Coupling the Calibrated GlobalLand30 Data and Modified PLUS Model for Multi-Scenario Land Use Simulation and Landscape Ecological Risk Assessment. *Remote Sens.* **2023**, *15*, 5186. [[CrossRef](#)]
32. Wu, X.X.; Liu, X.P.; Zhang, D.C.; Zhang, J.B.; He, J.Y.; Xu, X.C. Simulating mixed land-use change under multi-label concept by integrating a convolutional neural network and cellular automata: A case study of Huizhou, China. *GISci. Remote Sens.* **2022**, *59*, 609–632. [[CrossRef](#)]
33. Zhu, C.M.; Yuan, S.F.; Yang, L.X. Optimization and trade-off analysis of land use pattern in Hangzhou coupled with MOP and FLUS models. *Trans. Chin. Soc. Agric. Eng.* **2023**, *39*, 235–244.
34. Xie, G.; Zhen, L.; Lu, C.; Xiao, Y.; Chen, C. An expert knowledge-based approach to ecosystem service valorisation. *J. Nat. Resour.* **2008**, *5*, 911–919.
35. Li, X.; Fu, J.Y.; Jiang, D.; Lin, G.; Cao, C.L. Land use optimization in Ningbo City with a coupled GA and PLUS model. *J. Clean Prod.* **2022**, *375*, 134004. [[CrossRef](#)]
36. Jiang, Y.; Du, G.M.; Teng, H.; Wang, J.; Li, H.L. Multi-Scenario Land Use Change Simulation and Spatial Response of Ecosystem Service Value in Black Soil Region of Northeast China. *Land* **2023**, *12*, 962. [[CrossRef](#)]
37. Hasan, S.S.; Zhen, L.; Miah, M.G.; Ahamed, T.; Samie, A. Impact of land use change on ecosystem services: A review. *Environ. Dev.* **2020**, *34*, 100527. [[CrossRef](#)]
38. Tan, Z.; Guan, Q.; Lin, J.; Yang, L.; Luo, H.; Ma, Y.; Tian, J.; Wang, Q.; Wang, N. The response and simulation of ecosystem services value to land use/land cover in an oasis, Northwest China. *Ecol. Indic.* **2020**, *118*, 106711. [[CrossRef](#)]
39. Dong, K.; Wang, H.; Luo, K.; Yan, X.; Yi, S.; Huang, X. The Use of an Optimized Grey Multi-Objective Programming-PLUS Model for Multi-Scenario Simulation of Land Use in the Weigan-Kuche River Oasis, China. *Land* **2024**, *13*, 802. [[CrossRef](#)]
40. Tang, H.; Halike, A.; Yao, K.; Wei, Q.; Yao, L.; Tuheti, B.; Luo, J.; Duan, Y. Ecosystem service valuation and multi-scenario simulation in the Ebinur Lake Basin using a coupled GMOP-PLUS model. *Sci. Rep.* **2024**, *14*, 5071. [[CrossRef](#)]

41. Zhang, Y.; Naerkezi, N.; Zhang, Y.; Wang, B. Multi-Scenario Land Use/Cover Change and Its Impact on Carbon Storage Based on the Coupled GMOP-PLUS-InVEST Model in the Hexi Corridor, China. *Sustainability* **2024**, *16*, 1402. [[CrossRef](#)]
42. He, S.; Wang, J.; Li, J.; Sha, J.; Zhou, J.; Jiao, Y. Quantification and Simulation of the Ecosystem Service Value of Karst Region in Southwest China. *Land* **2024**, *13*, 812. [[CrossRef](#)]

**Disclaimer/Publisher’s Note:** The statements, opinions and data contained in all publications are solely those of the individual author(s) and contributor(s) and not of MDPI and/or the editor(s). MDPI and/or the editor(s) disclaim responsibility for any injury to people or property resulting from any ideas, methods, instructions or products referred to in the content.